

## Competition between sequential and direct paths in a two-photon transition

Béatrice Chatel, Jérôme Degert, Sabine Stock, and Bertrand Girard

Laboratoire de Collisions, Agrégats et Réactivité (CNRS UMR 5589), IRSAMC, Université Paul Sabatier, 31062 Toulouse Cedex, France

(Received 21 March 2003; published 22 October 2003)

Two-photon excitation of a quantum ladder system by a chirped pulse leads to interferences in the excited-state population, due to the phase differences between direct and sequential paths. First, based on an analytical approach, we separate and discuss the features of the contributions arising from these two paths. Then interferences with two intermediate levels are observed experimentally in atomic sodium vapor. Interplay between the two sequential paths leads to strongly contrasted oscillations and a great enhancement of the transition probability for some values of the chirp.

DOI: 10.1103/PhysRevA.68.041402

PACS number(s): 32.80.Wr, 32.80.Qk, 42.65.Re, 78.47.+p

Study of two-photon transitions with the aim to achieve high-resolution spectroscopy [1] or to maximize the excitation efficiency of a desired state has been an active field of research in the past decades. The first experiments on coherent two-photon effects were performed in 1972 by Shoemaker *et al.* [2] and since then theoretical and experimental studies have been performed on the one hand to improve spectroscopy [3] and on the other hand to control the final population transfer through achieving quantum interferences [4,5] or/and manipulating the coherent properties of the optical field [6].

Many results have been obtained in the high- [7] or intermediate-field regime involving adiabatic transfer in multilevel ladder climbing in atomic [8–10] or molecular systems [11,12]. In molecules, schemes based on chirped ultrashort pulses have been proposed and used to climb electronic ladders [13], vibrational ladders in direct [11,14] or Raman schemes [15], or even the rotational levels in a molecular centrifuge [16]. The advent of ultrafast lasers combined with pulse-shaping techniques has led to new schemes [17,18] where two-photon transitions representing the lowest-order nonlinear interaction are used as a benchmark system. In particular, Silberberg and co-workers [6,17] have shown that the two-photon absorption rate is maximized for transform-limited pulses only in the case of transitions without any resonant intermediate state. For transitions involving a nearly resonant intermediate state, an enhancement by a factor of 7 of the two-photon absorption rate in Rb vapor has been obtained by shaping the pulse [6]. Effectively the broad bandwidth of ultrashort lasers allows one to take advantage of interference effects between quantum paths in multiphoton transitions. Considering the simplest case of linearly chirped pulses where the laser frequency is regularly swept during the pulse, Noordam and co-workers [4] observed quantum interferences between sequential and direct two-photon transitions in rubidium. These interferences are due to the phase difference accumulated by various quantum paths, namely the direct nonresonant two-photon transition and sequential ladder climbing. They are observed as a function of the laser chirp. These interferences are related to, but of a different nature from, the two-photon versus two-photon interferences [19,20].

In this paper, we present an analytic derivation which allows us to mathematically distinguish the sequential and di-

rect contributions. The scheme is extended to the case of several intermediate states which provide as many sequential excitation paths and new interference possibilities. In particular, interferences between these sequential paths produce totally different patterns as compared to the sequential-direct interferences. This scheme is applied to the ( $3s \rightarrow 3p \rightarrow 5s$ ) ladder system in sodium vapor. Highly contrasted interferences are observed, as a direct consequence of this new interference scheme.

Let us consider an atomic system with three levels:  $|g\rangle$ ,  $|i\rangle$ , and  $|e\rangle$ , the ground, intermediate, and excited state.  $\omega_{ig}$ ,  $\omega_{ei}$ , and  $\omega_{eg}$  are the corresponding transition frequencies. This ladder system is excited by a weak femtosecond pulse  $\mathcal{E}(t)$ , which is linearly chirped and Gaussian-shaped.  $E(\omega)$  is the Fourier transform of  $\mathcal{E}(t)$  and is given by

$$E(\omega) = \sqrt{\pi} \mathcal{E}_0 T_0 e^{-(\omega - \omega_0)^2 T_0^2 / 4} e^{i\phi''(\omega - \omega_0)^2 / 2}, \quad (1)$$

where  $2T_0$  is the field-transform-limited temporal width (at  $1/e$ ),  $\delta\omega_L = 4/T_0$  is the field spectral width, and  $\phi''$  is the quadratic phase dispersion. The carrier frequency  $\omega_0$  is assumed to be on two-photon resonance ( $\omega_0 = \omega_{eg}/2$ ). The one-photon detuning  $\delta = \omega_{ig} - \omega_0$  is smaller than or comparable to the spectral bandwidth. The chirped pulse width given by:  $T_p = T_0 \sqrt{1 + (2\phi''/T_0^2)^2}$  is assumed here to be considerably shorter (picosecond scale) than all lifetimes (nanosecond scale) involved. The general expression of the excited-state amplitude due to a two-photon transition involving an intermediate resonant level  $|i\rangle$  can be written as [6]

$$a_e = -\frac{\mu_{ei}\mu_{ig}}{\hbar^2} \left[ \frac{1}{2} E(\omega_{ig}) E(\omega_{ei}) + \frac{i}{2\pi} \mathcal{P} \int_{-\infty}^{+\infty} d\omega \frac{E(\omega) E(\omega_{eg} - \omega)}{\omega - \omega_{ig}} \right], \quad (2)$$

where  $\mu_{ei}$  and  $\mu_{ig}$  are the dipole moment matrix elements and  $\mathcal{P}$  is the principal Cauchy value. Silberberg and co-workers [6] allocated the first term in Eq. (2) to the resonant contribution through the intermediate state and the second term to the off-resonance contributions. However, this second term includes contributions from the whole spectrum,

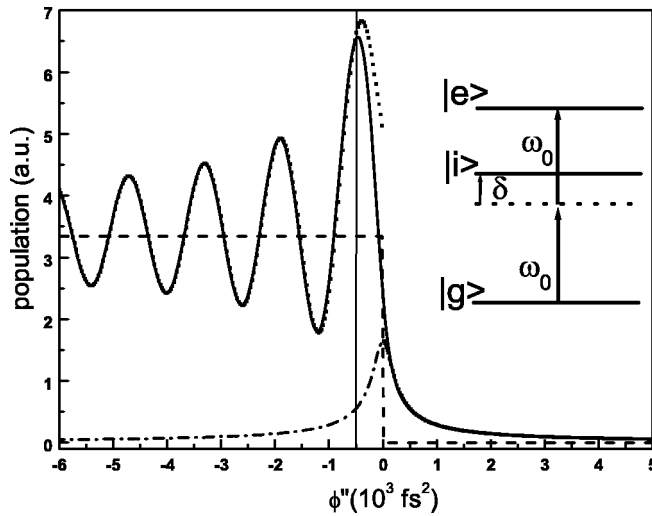


FIG. 1. Population of the excited state as a function of chirp for  $\delta > 0$ . Dashed line: sequential contribution  $|a_s|^2$  (dashed line); direct contribution  $|a_d|^2$  (dash-dotted line), total two-photon contribution  $|a_e|^2$  [using Eq. (2) (solid line) and Eq. (3) (squares)]. Inset: three-level system.  $\omega_0$  is the carrier frequency of the laser and  $\delta$  the detuning. The vertical line corresponds to  $\phi'' = -3\pi/4\delta^2$ .

involving also the one-photon resonance ( $\omega = \omega_{ig}$ ) with a significant weight. In the case of chirped pulses such that both sequential frequencies ( $\omega_{ig}$  and  $\omega_{ei}$ ) are separated in time

( $|\phi''| \gg 1/\delta^2$ ), it is shown below that the second term can be separated in two distinct contributions.

Even if general expressions can be derived for any field, the analytical expressions shown below [and in particular Eq. (3b)] are obtained with the Gaussian field given by Eq. (1). Two frequency ranges provide major contributions to the second term in Eq. (2), around  $\omega_0$  and  $\omega_{ig}$ , respectively. The first one results from the stationary phase approximation, and gives the direct two-photon transition amplitude. It corresponds to a small range of frequencies (width  $\approx 1/\sqrt{|\phi''|}$ ) centered on  $\omega_0$  that can fulfill the two-photon resonance condition. The second one is due to the pole in the principal Cauchy value, and provides a second significant contribution, identical to the sequential contribution already identified in Eq. (2). Finally, one obtains the probability amplitude  $a_e = a_s + a_d$ , with

$$a_s = -\frac{\mu_{ei}\mu_{ig}}{\hbar^2} E(\omega_{ei})E(\omega_{ig}) \frac{1 - \text{sgn}(\phi''\delta)}{2}, \quad (3a)$$

$$a_d = -\frac{\mu_{ei}\mu_{ig}}{\hbar^2} \frac{E^2(\omega_0)}{\delta\sqrt{2\pi T_0 T_p}} e^{-i(\theta+\pi)/2}, \quad (3b)$$

where  $a_s, a_d$  are the sequential and direct contributions, respectively, and  $\tan \theta = -2\phi''/T_0^2$ . Note that  $a_d$  corresponds exactly to the nonresonant excited-state amplitude [6] with a far off-resonance intermediate state.

As shown in Fig. 1,  $|a_d|^2$  (dash-dotted) is maximized for transform-limited pulses ( $\phi'' \approx 0$ ) and evolves as  $\sim 1/T_p$ , with a full width at half maximum equal to  $T_0^2\sqrt{3}$ .  $a_s$  consists

of two terms of equal magnitude arising from the first part of Eq. (2) clearly identified previously, and from the principal value. This sequential contribution is either twice the first term of Eq. (2), or vanishes, depending on the sign of  $\phi''\delta$ . For a given sign of  $\phi''\delta$ , its magnitude is constant. This means intuitively that the frequencies should arrive in the correct order ( $\omega_{ig}$  before  $\omega_{ei}$ ) to have a significant sequential contribution: excitation of the intermediate state  $|i\rangle$  followed by excitation from  $|i\rangle$  to  $|e\rangle$  (see the dressed state picture explanation below). The sequential contribution contains a phase factor  $e^{i\phi''\delta^2}$ , arising from the electric field [see Eq. (1)]. The corresponding probability is a steplike function (dashed line in Fig. 1) depending only on the power spectrum at each one-photon transition. The total probability  $|a_e|^2$  exhibits strong interferences due to the phase difference accumulated between both paths. In Fig. 1, the analytic approximation of  $|a_e|^2$  [Eq. (3)] and the numerical integration of Eq. (2) are plotted with squares and a solid line, respectively (for  $\delta > 0$  and  $\delta/\delta\omega_L \approx 0.5$ ). Both fit perfectly except for the small region around zero chirp ( $|\phi''| \leq 1/\delta^2$ ), where our approximation is not valid. For  $\phi'' > 0$ ,  $|a_e|^2$  has the same behavior as  $|a_d|^2$ . It corresponds to the population transferred by two photons with the same energy  $\hbar\omega_{eg}/2$ . On the other hand, for  $\phi'' < 0$  the population oscillates around  $|a_s|^2$ . From Eq. (3), the period of the oscillations is equal to  $\phi''_{2\pi} = 2\pi/\delta^2$ . The first maximum is reached when both amplitudes have nearly the same phase factors, i.e., for  $\phi'' \approx -3\pi/4\delta^2$ .

These interferences were first observed experimentally by Noordam and co-workers in Rb [9], although the relative contributions of the sequential and direct paths were not calculated. However, this analytic result stresses the difference of behavior between direct and sequential paths as a function of the chirp: a rapid decay for the direct contribution compared to a constant magnitude (for the correct sign of  $\phi''$ ) and a phase factor of  $\phi''\delta^2$  for the sequential one. Adding new sequential paths leads to multiple interferences and increases the possibilities of improving the interference contrast. For instance, this is obtained when the different detunings  $\delta_k = \omega_{ikg} - \omega_0$  keep close together. The direct path is not qualitatively changed, only  $\mu_{ei}\mu_{ig}/\delta$  should be replaced by  $\sum_k \mu_{ei}\mu_{ikg}/\delta_k$ . In the simplest case of two intermediate states, interferences occur between three paths, as can easily be seen from the dressed states picture. The dressed atomic states are  $|a, n\rangle$ , where  $|a\rangle$  is an atomic state and  $|n\rangle$  the photon number state, as shown in Fig. 2. A given manifold of neighboring energy consists of  $|g, n+1\rangle$ ,  $|i_k, n\rangle$ , and  $|e, n-1\rangle$ . The dashed lines represent the diabatic states and the solid lines the quantum paths (including the atom-field coupling). For a positively (negatively) chirped pulse, the temporal evolution of the system corresponds to a traversal of the diagram from left to right (right to left). At each crossing, the wave packet splits into two components of relative magnitude depending on the coupling strength. Here in the weak-field regime, the major component remains on the diabatic curve. The two sequential paths (1) and (2) correspond to two successive one-photon transitions. They can be followed only for negative chirp (for  $\delta > 0$ ). Paths (3) and (4) are the

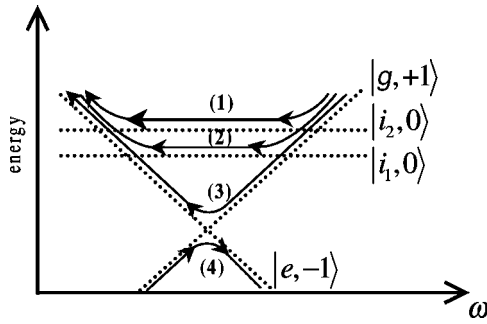


FIG. 2. Dressed states picture of a ladder system with two intermediate states. The arrows indicate the different paths.

direct two-photon transitions for negative and positive chirp, respectively. Note that for chirps small enough ( $|\phi''| \leq T_0^2$ ), all the frequencies can be considered to be simultaneously present, and the dressed level picture is not appropriate to explain the observations. Then the distinction between the sequential and direct two-photon processes is not relevant.

As qualitatively explained by Noordam and co-workers [4], the relative phase between the paths is given by the product of the chirp rate by the enclosed area delimited by these paths in the dressed state diagram. This leads to oscillations of the final population as a function of the chirp. These result from the beats of three interference periods: two rapid ones due to the interferences of sequential paths (1) and (2) with the direct path (3), and one slow one corresponding to interferences between path (1) and (2) (in case of a splitting small compared to the one-photon detunings  $\delta_k$ ). The probability of each path depends on the strength of the coupling at the crossing, which is proportional to the laser electric field amplitude and the respective dipole moments. This latter leads to highly contrasted interference (in the case of balanced excitation paths) with a chirp-independent amplitude, whereas the sequential-direct interference amplitude decreases rapidly with  $|\phi''|$ . Moreover, it depends critically on the value of  $\delta_k/\delta\omega_L$ . This explains the relatively small interference amplitude in Noordam's experiment, where  $\delta/\delta\omega_L \approx 0.25$  (compared to this present study, where  $\delta/\delta\omega_L \approx 0.5$ ): Therefore for the chirp corresponding to the first maximum ( $\approx -3\pi/4\delta^2$ ), the direct two-photon magnitude has already strongly decreased. This dressed atom picture does not allow us to determine the absolute position of the interference pattern with respect to  $\phi''=0$ , and in particular, the phase shift of  $3\pi/4$  between the direct two-photon path and the sequential paths.

In order to illustrate this scheme involving two sequential paths, an experiment has been performed in sodium atoms. The ( $3s$ - $5s$ ) two-photon transition (at 603 nm) is excited with a chirped pulse. The laser bandwidth allows us to excite the sequential (at 589 and 615 nm) and the direct two-photon transitions. The ( $4p$ - $3s$ ) fluorescence is recorded as a function of chirp. This two-photon transition involves two intermediate states  $3p$  ( ${}^2P_{1/2}$  and  ${}^2P_{3/2}$ ) and one excited state  $5s$ ,  ${}^2S_{1/2}$ . The one-photon detunings are close:  $\delta_1 \approx 0.067$  rad fs $^{-1}$  and  $\delta_2 \approx 0.070$  rad fs $^{-1}$  for  ${}^2P_{1/2}$  and  ${}^2P_{3/2}$ , respectively.

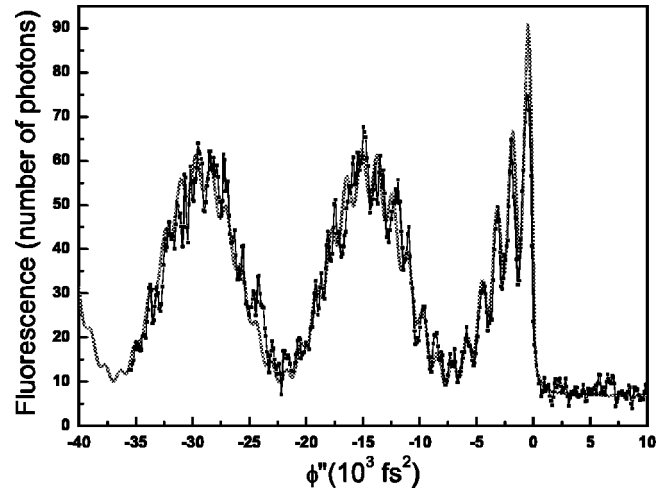


FIG. 3.  $4p$ - $3s$  fluorescence as a function of chirp. Black line and squares: experiment; gray line: theory.

The laser system is based on a conventional Ti:sapphire laser with chirped pulse amplification (Spitfire Spectra Physics) which supplies 800  $\mu$ J-130 fs-1 kHz 795 nm pulses. A fraction of the energy feeds a homemade Noncollinear Optical Parametric Amplifier (NOPA) [21], without compression, which delivers pulses of 10  $\mu$ J, 28 nm bandwidth centered around 603 nm. To vary the chirp  $\phi''$  on the interval  $[-40\,000$  fs $^2$ , 40 000 fs $^2$ ] with 100 fs $^2$  steps, we combine glass rods (4 cm SF58, 6 cm SF10) with a tunable double pass grating pair (600 grooves/mm). The pulse is slightly focused into a sealed cell containing natural sodium with a pressure of  $1.7 \times 10^{-4}$  Pa. The  $4p \rightarrow 3s$  fluorescence signal at 330 nm is collected by 18 optical fibers and detected by a photomultiplier with photon counting. The signal was monitored as a function of the grating's distance, which is essentially proportional to the chirp.

Figure 3 presents the experimental result compared with a theoretical simulation based on the numerical calculation of the excited-state probability as derived from Eq. (2), summing over both  $3p$  intermediate states ( ${}^2P_{1/2}$  and  ${}^2P_{3/2}$ ). In the calculation, the complete phase of the laser pulse is included instead of a pure quadratic phase to take into account the higher-order dispersion terms. However, for the sake of simplicity, the results are plotted as a function of the chirp  $\phi''$  (the effect of the higher-order dispersion terms will be treated in more detail elsewhere [22]). The agreement between theory and experiment is excellent without any adjustment except for a normalization factor. The high contrast and the beat of slow and fast oscillations are clearly observable for negative chirp. As described above, for positive chirp [corresponding to  $\text{sgn}(\phi''\delta)=1$ ] the signal is rapidly decreasing and is only due to the direct two-photon transition. The sharp step corresponds to the passage of the pulse around the zero chirp. Considering Eq. (3), for  $\delta_1 \approx \delta_2$ , the first maximum of the interference pattern appears at  $\phi''_k = -3\pi/4\delta_k^2 \approx -500$  fs $^2$  in our case ( $\phi''_1 \approx -525$  fs $^2$  and  $\phi''_2 \approx -480$  fs $^2$ ). The enhancement of the population transfer between this chirp and a transform-limited pulse is about a

factor of 3. The combination of slow and fast oscillations leads to a maximum enhancing factor of 20 between the minimum at  $\phi'' \simeq -7500 \text{ fs}^2$  and the maximum at  $\phi'' \simeq -500 \text{ fs}^2$ . As described above, the oscillation periods are easy to deduce as well from the analytic expression as from the dressed states picture. The two fast periods are very close together and equal to about  $1272 \text{ fs}^2$  for the  ${}^2P_{3/2}$  and  $1399 \text{ fs}^2$  for the  ${}^2P_{1/2}$ . These are extremely well reproduced experimentally with an average small period of  $1334 \text{ fs}^2$ . The large period is due to the interferences between the two sequential paths (1) and (2) and is equal to  $14\,125 \text{ fs}^2$ , corresponding to the experimental result. The contrast of the fast oscillations decreases as a function of the chirp experimentally as well as theoretically, whereas that of the slow oscillations keeps a constant value of  $\sim 0.75$ .

Finally, the slow oscillations can also be regarded as resulting from a wave packet oscillating between a bright and a dark state. This wave packet, which is a coherent superposition of the two intermediate states, is created by the first sequential transition at  $t_i = (\delta_1 + \delta_2)\phi''/2$  and detected when the laser frequency reaches the second sequential transition at  $t_f = -(\delta_1 + \delta_2)\phi''/2$ . The accumulated relative phase between the two levels is  $(t_f - t_i)\Delta E/\hbar = (t_f - t_i)(\delta_2 - \delta_1) = (\delta_2^2 - \delta_1^2)\phi''$  as calculated above. The dark state  $|L = 1, M_L = \pm 1\rangle$  cannot be excited towards the final state without any change of the laser polarization during the pulse. This explains the much higher contrast observed here compared to previous spin precession studies [23].

We have presented in this paper a study of multipath interferences in quantum ladder climbing. A new analytic expression of the competition of sequential and direct contributions in a two-photon transition with chirped pulses has been derived. This expression allows us to separate them clearly and throws new light on ladder-climbing experiments. This result clearly demonstrates the difference of behavior between these two contributions and stimulated a new experiment where two intermediate states are involved. Highly contrasted interferences between two sequential quantum paths have been observed in excellent agreement with theory. Finally, the combination of linear chirp and more complex pulse shapes [26] in two-photon transitions with several intermediate states could be implemented to enhance the final population in the low-field regime. This scheme involving a two-photon transition in sodium represents a particular interest for the polychromatic artificial star project [24]. Adiabatic transfer is difficult to achieve at 100 km distance, and optimizing the excitation efficiency in the weak- or intermediate-field regime seems more appropriate [25].

We sincerely acknowledge Jean-Paul Pique for fruitful discussions on the artificial star project and the loan of the sodium cell. We also acknowledge financial support from the European Union (Contract No. HPRN-CT-1999-00129, COCOMO). We enjoyed fruitful and stimulating discussions with the late G. Grynberg.

- 
- [1] F. Biraben *et al.*, Phys. Rev. Lett. **32**, 643 (1974).  
 [2] R.L. Shoemaker *et al.*, Phys. Rev. Lett. **28**, 1430 (1972).  
 [3] J.E. Bjorkholm *et al.*, Phys. Rev. Lett. **33**, 128 (1974).  
 [4] P. Balling *et al.*, Phys. Rev. A **50**, 4276 (1994).  
 [5] E. Cormier *et al.*, Phys. Rev. A **59**, 3736 (1999).  
 [6] N. Dudovich *et al.*, Phys. Rev. Lett. **86**, 47 (2001).  
 [7] R.R. Jones, Phys. Rev. Lett. **74**, 1091 (1995).  
 [8] J. Oreg *et al.*, Phys. Rev. A **32**, 2776 (1985).  
 [9] B. Broers *et al.*, Phys. Rev. Lett. **69**, 2062 (1992).  
 [10] Y.B. Band, Phys. Rev. A **50**, 5046 (1994); N.V. Vitanov, J. Phys. B **31**, 709 (1998); R. Marani *et al.*, *ibid.* **32**, 711 (1999).  
 [11] S. Chelkowski *et al.*, Phys. Rev. Lett. **65**, 2355 (1990).  
 [12] J.S. Melinger *et al.*, J. Chem. Phys. **95**, 2210 (1991).  
 [13] A. Assion *et al.*, Chem. Phys. Lett. **259**, 488 (1996); B. Garraway *et al.*, Phys. Rev. Lett. **80**, 932 (1998); S. Kallush *et al.*, Phys. Rev. A **61**, 041401 (2000); B.Y. Chang *et al.*, J. Chem. Phys. **113**, 4901 (2000).  
 [14] D.J. Maas *et al.*, Chem. Phys. Lett. **290**, 75 (1998); S. Guérin, Phys. Rev. A **56**, 1458 (1997); T. Witte *et al.*, J. Chem. Phys. **118**, 2021 (2003).  
 [15] S. Chelkowski *et al.*, J. Raman Spectrosc. **28**, 459 (1997); J.C. Davis *et al.*, J. Chem. Phys. **110**, 4229 (1999).  
 [16] D.M. Villeneuve *et al.*, Phys. Rev. Lett. **85**, 542 (2000).  
 [17] D. Meshulach *et al.*, Nature (London) **396**, 239 (1998).  
 [18] T. Hornung *et al.*, Appl. Phys. B: Lasers Opt. **71**, 277 (2000).  
 [19] Z.D. Chen, P. Brumer, and M. Shapiro, Chem. Phys. Lett. **198**, 498 (1992); J. Chem. Phys. **98**, 6843 (1993).  
 [20] S.T. Pratt, J. Chem. Phys. **104**, 5776 (1996).  
 [21] E. Riedle *et al.*, Appl. Phys. B: Lasers Opt. **71**, 457 (2000).  
 [22] B. Chatel *et al.* (unpublished).  
 [23] C. Nicole *et al.*, Phys. Rev. A **60**, R1755 (1999); S. Zamith *et al.*, Eur. Phys. J. D **12**, 255 (2000); E. Sokell *et al.*, J. Phys. B **33**, 2005 (2000).  
 [24] R. Foy *et al.*, Astron. Astrophys., Suppl. Ser. **111**, 569 (1995).  
 [25] J. Biegert *et al.*, Opt. Lett. **25**, 683 (2000); Phys. Rev. A **67**, 043403 (2003).  
 [26] J. Degert, W. Wohlleben, B. Chatel, M. Motzkus, and B. Girard, Phys. Rev. Lett. **89**, 203003 (2002); J.B. Ballard, H.U. Stauffer, E. Mirowski, and S.R. Leone, Phys. Rev. A **66**, 043402 (2002).